

CIRCUS: an MDA platform for clinical image analysis in hospitals

Yukihiro Nomura¹, Naoto Hayashi², Yoshitaka Masutani^{1,3},
Takeharu Yoshikawa², Mitsutaka Nemoto¹, Shouhei Hanaoka¹,
Soichiro Miki³, Eriko Maeda², and Kuni Ohtomo^{1,3}

¹ Department of Radiology, The University of Tokyo Hospital,
7-3-1 Hongo, Bunkyo-ku, Tokyo 113-8655, Japan

² Department of Computational Diagnostic Radiology and Preventive Medicine,
22nd Century Medical and Research Center, The University of Tokyo Hospital
7-3-1 Hongo, Bunkyo-ku, Tokyo 113-8655, Japan

³ Division of Radiology and Biomedical Engineering, Graduate School of Medicine,
The University of Tokyo, 7-3-1 Hongo, Bunkyo-ku, Tokyo 113-8655, Japan
`nomuray-tyky@umin.ac.jp`

Abstract. For mass image data analysis in hospitals, we have built an integrated platform for the development and assessment of various types of image analysis software such as computerized detection of lesions. It mainly consists of a set of clinical image databases, and a clinical server with web-based interfaces for launching analysis software and for viewing and evaluating analysis results. The image databases are employed for the registration of a sufficient number of clinical cases for machine learning in computer-assisted detection/diagnosis (CAD) software development. In addition, the clinical server collects data for evaluating the interpretation performance of radiologists as well as that of the CAD software.

Keywords: computer-assisted detection/diagnosis (CAD), image database system, web-based clinical server, on-line learning

1 Introduction

A large number of images are generated by imaging devices in hospitals. The number of images is usually from 300 to 500 (and sometimes over 1,000) per examination and is increasing year by year. Hence, the workload of radiologists has been increasing. In addition, there are differences between the interpretation performance of radiologists. Therefore, computer-assisted detection/diagnosis (CAD) software is expected to assist radiologists.

The development of CAD software involves a cycle of algorithm development, software implementation, clinical use, and refinement of the algorithm and the software based on clinical evaluation. This cycle is expected to accelerate the development of CAD software. However, there are currently problems in CAD software development.

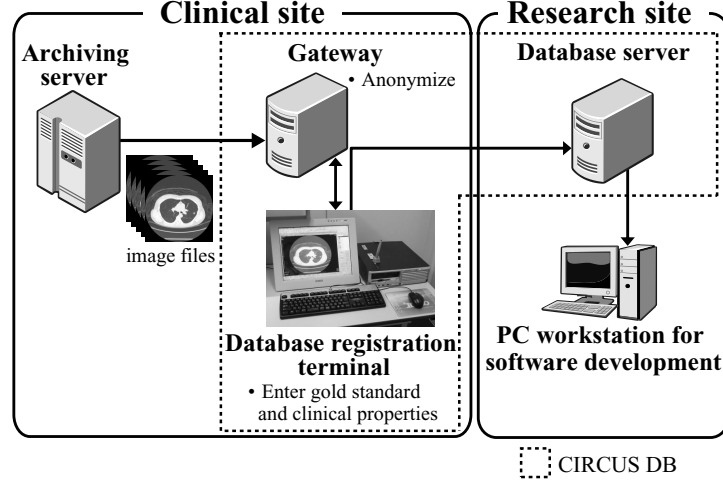


Fig. 1. Configuration of CIRCUS DB for collecting clinical cases with pixel-based gold standard data sets. CIRCUS DB includes a gateway, a database registration terminal, and a database server.

In algorithm development, a sufficient number of clinical cases are required to ensure the higher reliability of CAD software. In addition, the database must include pixel-based gold standard data sets for supervised learning in CAD software.

The clinical use of a CAD system requires on-line processing in the clinical image network, the retrieval of images from an imaging device or an archiving server, and the display of results obtained from the CAD software on interpretation terminals. In recent years, several research groups have reported CAD servers based on on-line processing of CAD software [1–4], which are aimed at improvement of diagnostic workflow and at clinical decision support. For example, Martinelli, et al. [4] reported an integrated platform dedicated to chronic heart failure, including web-based interfaces for analyzing echocardiograms and a knowledge-based decision support system. A commercial CAD server (syngo.via; Siemens Healthcare, Erlangen, Germany) has also been released. However, these systems might lack viewpoints of tuning and improvement of CAD software performance in an efficient way.

Clinical images have different properties depending on imaging devices, in terms of pixel size, slice thickness, signal-to-noise ratio, field of view, and others. It is important to adapt CAD software to various imaging configurations based on incremental learning. Previously, CAD software has been developed for off-line applications [5]. Thus, if new clinical cases are collected, relearning incorporating the additional cases must be carried out. However, it is difficult to collect additional cases due to the protection of personal information in hospitals. Therefore, a strategy for the on-line learning of CAD software in clinical environment is important. To refine or adapt CAD software based on on-line

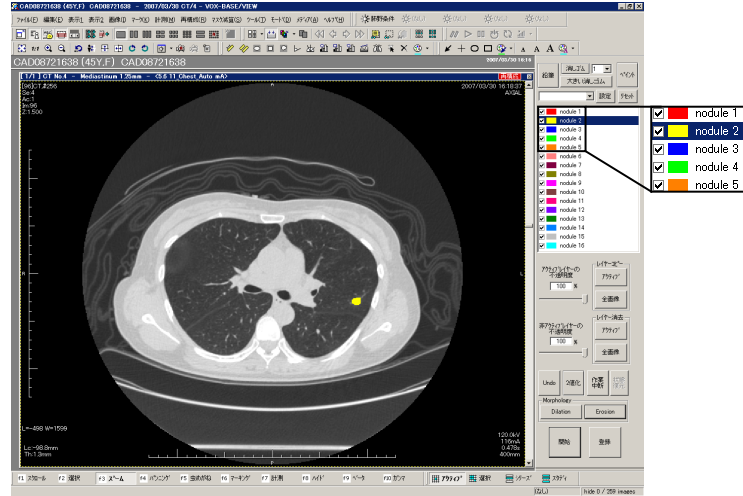


Fig. 2. Interface for pixel-based gold standard labeling. The arrow indicates the labeled gold standard. Gold standard is painted in colors depending on the categorization of each region.

learning, it is required to evaluate whether or not the results obtained from CAD software are appropriate on the basis of a clinical diagnosis and to realize on-line learning based on evaluations.

To solve the above problems in CAD software development, we have been building an integrated system for the development, clinical use, evaluation, and refinement of CAD software as a mass data analysis (MDA) platform for clinical image analysis in hospitals. The system was named CIRCUS (clinical infrastructure for radiologic computation of united solutions).

2 System description

We have built two types of subsystem for CAD software development. First, we built an image database system with an interface for pixel-based gold standard labeling to effectively collect a sufficient number of clinical cases with pixel-based gold standard data sets. In addition, we also built a web-based clinical server to realize the on-line processing of CAD software and interfaces for evaluating CAD results and for on-line learning. We named the image database system CIRCUS DB and the web-based clinical server CIRCUS CS.

2.1 CIRCUS DB (image database system)

CIRCUS DB includes a gateway, a database registration terminal, and a database server (Fig. 1). The gateway retrieves image files from an archiving server based on requests from the database registration terminal, and then anonymizes the

- size
- type
 - solid
 - mixed GGO
 - pure GGO
- location
 - isolated
 - juxta-pleural
 - juxta-vascular
- with calcification
- with cavity
- with fat
- free comment

Fig. 3. Interface for entry of clinical properties in database of lung nodules. The properties of lung nodules are size, type, location, calcification, cavity, and fat, and an additional space is provided for comments (GGO: ground glass opacity).

image files. At the database registration terminal, pixel-based gold standard and clinical properties are entered using interface windows. After these processes, anonymized image files with gold standard and clinical properties are registered in the database server. At the research site, image files with gold standard data are retrieved upon request for software development. Clinical properties are also retrieved as comma-separated values (CSV) files.

Interfaces for labeling pixel-based gold standard and for entering clinical properties. Pixel-based gold standard is semiautomatically or manually labeled on each 2D image using a mouse or pen tablet. Figure 2 shows an interface for gold standard labeling. Gold standard is painted in colors depending on the categorization of each region. For example, benign lung nodules are painted in yellow, and malignant lung nodules are painted in red. Labeled gold standard data are saved as digital imaging and communications in medicine (DICOM) overlays with up to 16 layers. After that, clinical properties are entered using an interface window (Fig. 3). Various clinical properties are set for each database. For example, the properties of lung nodules are their size, type, location, calcification, cavity, and fat, and an additional space is provided for comments.

2.2 CIRCUS CS (clinical server with web interface)

Figure 4 shows the configuration of CIRCUS CS. The processing procedures of CIRCUS CS are described as follows.

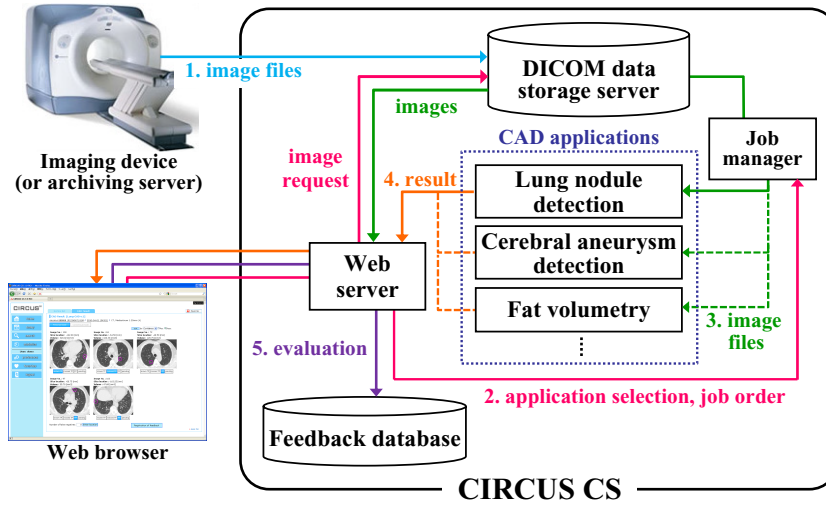


Fig. 4. Configuration of CIRCUS CS for on-line processing of CAD software and evaluating CAD results. CIRCUS CS includes a DICOM data storage server, a job manager, a web server, and a feedback database. CAD applications are provided as plug-ins of CIRCUS CS.

1. Image files are transferred from an imaging device or an archiving server to a DICOM data storage server.
2. The user selects a CAD application via a web browser and then registers a job order.
3. The job manager process the selected application.
4. The results obtained from the CAD application and interfaces for evaluation (clinical feedback) are displayed as a web page.
5. Radiologists evaluate the results from the CAD application on the basis of a diagnostic decision, and the entered evaluations are registered in the feedback database.

CAD applications are provided as plug-ins of CIRCUS CS. Our CAD applications are outlined below.

- Lesion detection applications: cerebral aneurysm detection in magnetic resonance (MR) angiograms [6], lung nodule detection in chest computed tomography (CT) images [7], skin lesion detection in whole-body ^{18}F -fluorodeoxy-glucose positron emission tomography/computed tomography (FDG-PET/CT) images [8]
- Visualization application: virtual straightening of spine in whole-body CT images [9]
- Measurement application: volumetry of visceral fat tissue (VAT) and subcutaneous fat tissue (SAT) in whole-body CT images

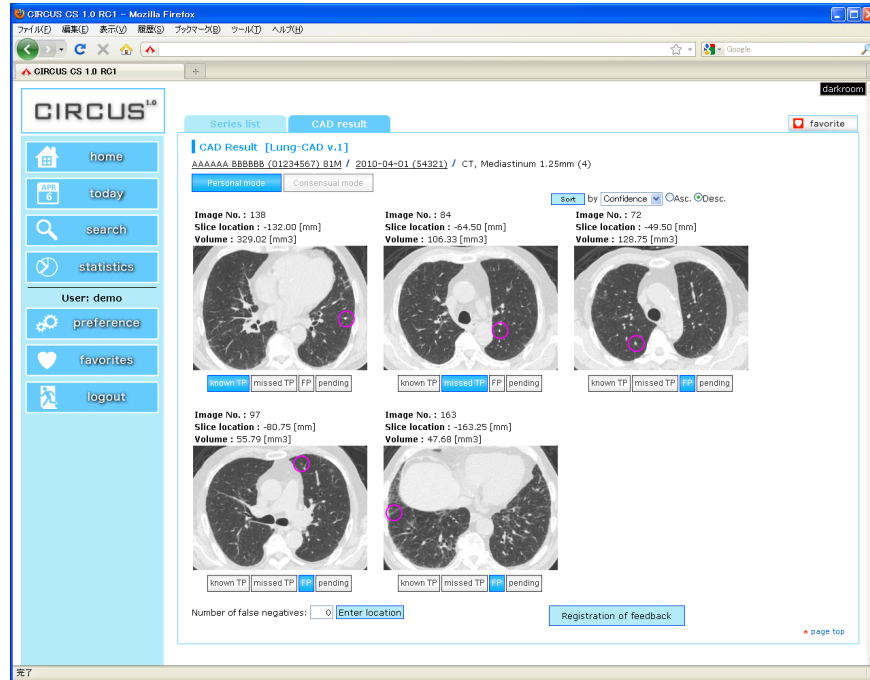


Fig. 5. Result of lung nodule detection in CT images. The center slice of the lesion candidate and radio buttons (as a feedback interface) are displayed for each lesion candidate. Circles indicate the locations of lesion candidates.

The user logs in to CIRCUS CS using his/her individual user ID and password. The individual login enables us to adjust a set of displayed lesion candidates adaptively for each user. In addition, it also enables the collection of personal diagnostic decision data for each radiologist. On the basis of the collected data, the interpretation performance of the radiologist can be evaluated.

Figure 5 shows a result of lung nodule detection in chest CT images. The center slice of the lesion candidate and radio buttons (as a feedback interface) are displayed for each lesion candidate. Lesion candidates are displayed in descending order of likelihood, and the number of displayed lesion candidates is adjusted by each user. In Fig. 5, the top five lesion candidates are displayed. Hereafter, the displayed lesion candidates are referred to “displayed candidates”, and other potential candidates are referred to “undisplayed candidates”.

2.3 Interfaces for clinical feedback

Radiologists evaluate the results obtained from the CAD application on the basis of a diagnostic decision. The feedback entry in our system includes two stages: a personal entry and a consensual entry (Fig. 6). In the personal entry,

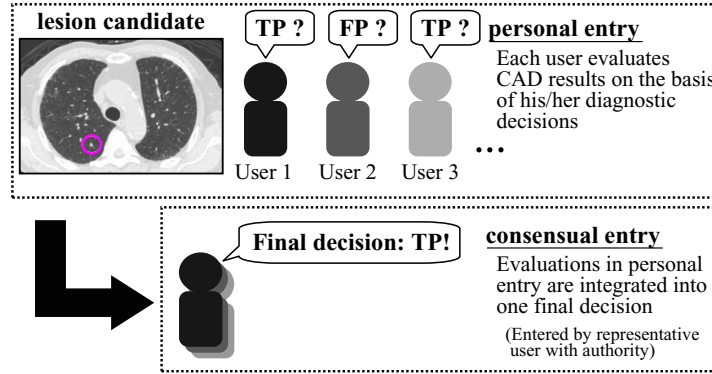


Fig. 6. Two stages of clinical feedback entry.

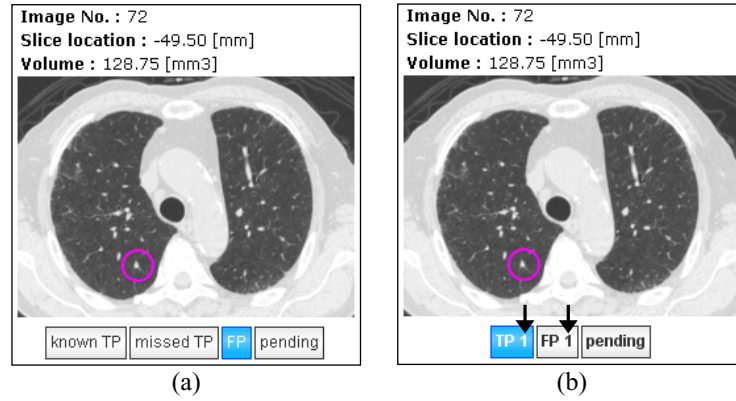


Fig. 7. Radio buttons used to classify displayed candidates. (a) Personal entry, (b) consensual entry. The arrows indicate the number of users entered in the personal entry.

each radiologist can evaluate the result obtained from the CAD application. Evaluations in the personal entry by two radiologists (or more) are integrated into one final decision as the consensual entry. We have implemented two types of interface for clinical feedback entry, which are for lesion detection applications and for visualization applications.

Interfaces for lesion detection applications. The interfaces for lesion detection applications include radio buttons to classify displayed candidates and an interface for entering the locations of false negative (FN). Figure 7 (a) shows radio buttons used to classify displayed candidates in the personal entry. Each displayed candidate is classified as follows:

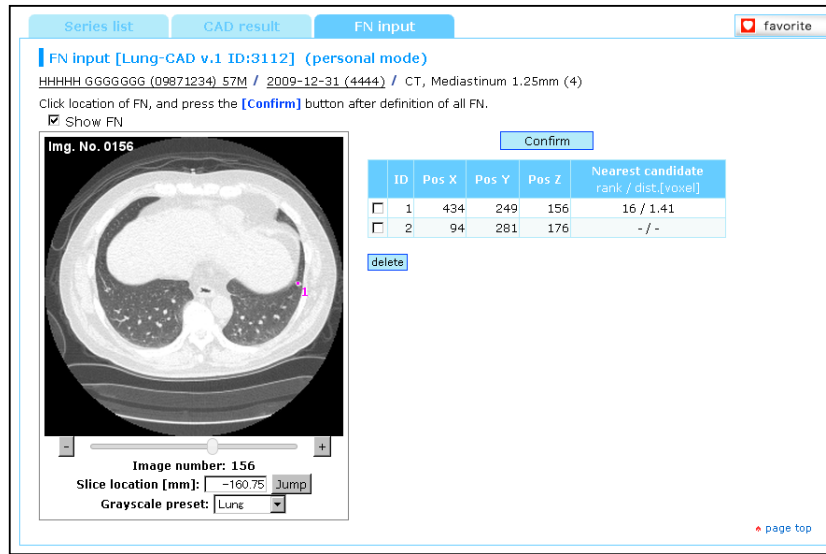


Fig. 8. Interface for used entering FN locations. The location of each FN is entered by clicking on the left 2D image. The right table shows the coordinates of the FNs and the existence of undisplaced candidate.

- known true positive (TP): lesion detected by radiologist's interpretation without CAD application
- missed TP: lesion missed in radiologist's interpretation without CAD application
- false positive (FP): false positive of the CAD application
- pending: difficult to classify into a TP or FP

Figure 7 (b) shows radio buttons used in the consensual entry. The number of radiologists at the personal entry is displayed in the radio buttons (arrows in Fig. 7 (b)). In the consensual entry, known TPs and missed TPs are usually integrated into TPs.

In the interface used for entering the location of FN, a 2D image including an FN is first selected using a slider control (Fig. 8). After clicking on the location of FN, its coordinates and the existence of undisplaced candidate are added to a table.

Accumulated clinical feedback, which includes the classification of displayed candidates and the locations of FNs, can be used to evaluate the performance of the CAD software and to refine the software. For radiologists, collecting data on personal entry including the number of missed lesions makes it possible to investigate individual differences in interpretation performance. We have also implemented an interface showing the interpretation characteristics of each user based on his/her clinical feedback (Fig. 9). The interface shows a table of classifications of lesion candidates and scatter plots of the classification results. The



Fig. 9. Interface showing interpretation characteristics in lung nodule detection. The interface shows a table of classifications of lesion candidates and scatter plots of the classification results. Each classification in the scatter plots can be shown or hidden using check boxes (dashed box).

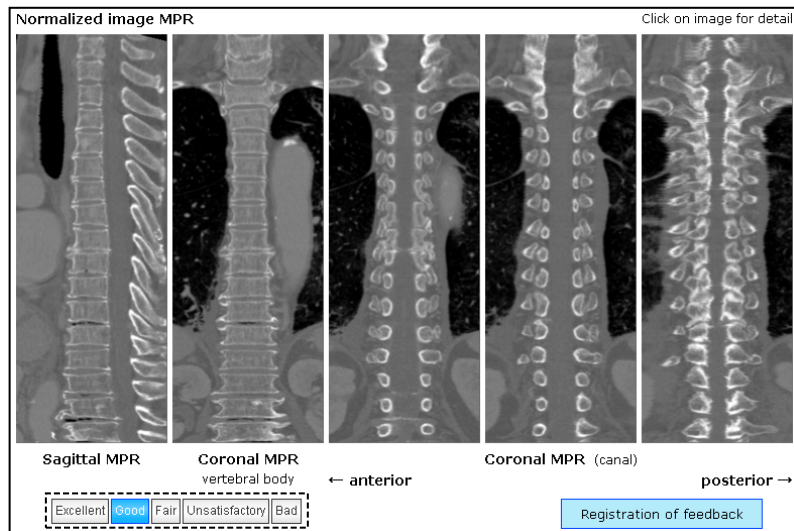


Fig. 10. Result of virtual straightening of spine in whole-body CT images with feedback interface for entering visual score (dashed box).

Table 1. Average times required for data retrieval at research site.

Type of database	Image type	Size	Time [sec]	File size [MB]	
				original image	gold standard
Cerebral aneurysm	MR(A)	512×512×132	45	69.2	34.6
Lung nodule	CT	512×512×250	80	131.0	65.5
Skin lesion	CT*	512×512×275	95	144.2	72.1
	CT**	512×512×717	180	375.9	-
	PET	128×128×275	10	9.0	-
Visceral space	CT	512×512×717	240	375.9	375.9

* Slice thickness: 3.75mm (for gold standard labeling)

** Slice thickness: 1.25mm (for processing)

Table 2. Average times required for transfer of image files and processing of CAD applications.

CAD application	Image type	Size	No. of images	Time for transfer [sec]	Time for processing [sec]	Total [sec]
Cerebral aneurysm detection	MR(A)	512×512	152	15	45	60
Lung nodule detection	CT	512×512	250	20	185	205
Skin lesion detection	CT	512×512	717	50	270	330
	PET	128×128	275	10		
Vertebral deformity analysis	CT	512×512	717	50	220	270
Volumetry of VAT and SAT	CT	512×512	717	50	380	430

coordinates of the scatter plots are normalized by target volumes. Each classification in the scatter plots can be shown or hidden using check boxes.

Interface for visualization applications. Figure 10 shows an example of a feedback interface for visualization applications. The user enters a visual score using radio buttons. The visual score is divided into five levels: excellent, good, fair, unsatisfactory, and bad.

3 Results

The specifications of our platform including the databases and servers are shown below.

- Gateway: Intel Dual Xeon 1.86 GHz dual processor with 3 GB RAM, and Microsoft Windows Server 2003 operating system
- Database registration terminal: Intel Pentium D 3.40 GHz with 2 GB RAM, and Microsoft Windows XP Professional operating system
- Database server: Intel Dual Xeon 1.86 GHz dual processor with 3 GB RAM, Microsoft Windows Server 2003 operating system, and MySQL 5.0.45
- Clinical server: Intel Quad Xeon 2.0 GHz with 4 GB RAM, Microsoft Windows Server 2003 operating system, Apache 2.2.15, Open SSL 0.9.8m, PostgreSQL 8.4.4, and DCMTK 3.5.4 [10]

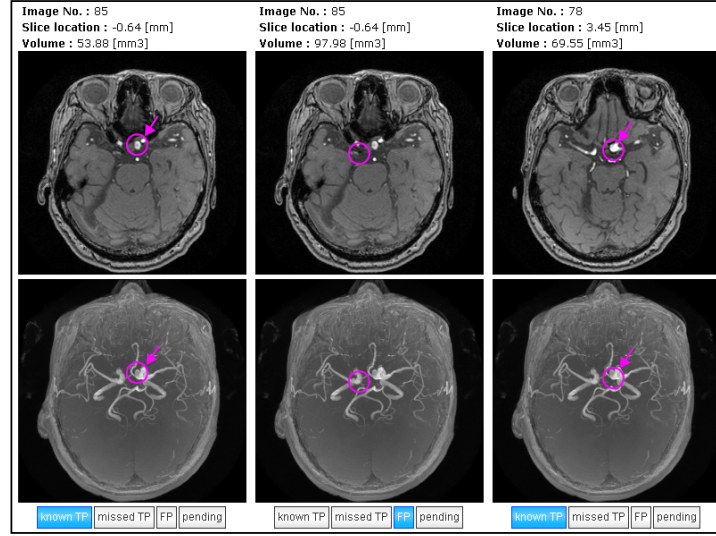


Fig. 11. Result of cerebral aneurysm detection in MR angiograms. The upper images show the center slice of the displayed candidate, the lower images show the maximum-intensity projection. The circles indicate the location of the lesion candidate, and the circles with an arrow indicate the detected cerebral aneurysm.

We built four types of image databases: 1) cerebral aneurysms in MR angiograms, 2) lung nodules in chest CT images, 3) skin lesions detection in whole-body FDG-PET/CT images, and 4) visceral spaces in whole-body CT images. The present databases included 1,061 cases of cerebral aneurysms, 111 cases of lung nodules, 37 cases of skin lesions, and 26 cases of visceral spaces. In the database for lesion detection applications, the average time required for gold standard labeling, data transfer, and registration was 1.5 to 8 minutes per case, depending on the number, size, and shape of lesions. In contrast, it took about eight hours to enter the gold standard of a visceral space, since the labeling of gold standard data includes that of regions of the diaphragm, liver, spleen, abdominal aorta, kidney, and other regions as well as those of the visceral space.

At the research site, the average time required for data retrieval was 1 to 5 minutes per case (Table 1). We developed CAD applications based on clinical cases registered in CIRCUS DB. The applications were cerebral aneurysm detection in MR angiograms (Fig. 11), lung nodule detection in chest CT images (Fig. 5), skin lesion detection in whole-body FDG-PET/CT images (Fig. 12), virtual straightening of spine in whole-body CT images (Fig. 10), and volumetry of VAT and SAT in whole-body CT images (Fig. 13).

The clinical server with our CAD applications was utilized in our hospital. The time required for the transfer of image files and the processing of CAD applications ranged from 1 to 7 minutes per case, depending on the number of image files and the type of CAD application (Table 2). Table 3 shows the

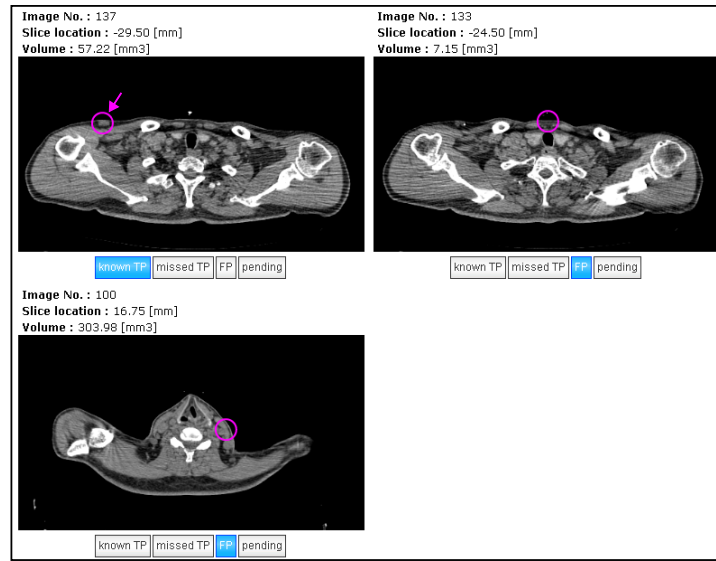


Fig. 12. Result of skin lesion detection in whole-body FDG-PET/CT images. The center slice of the displayed candidate is displayed in a CT image. The circles indicate the location of the lesion candidate, and the circle with an arrow indicates the detected skin lesion.

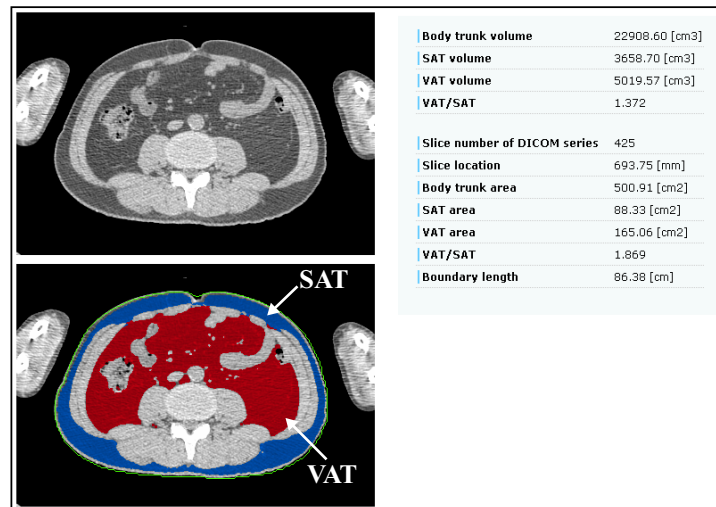


Fig. 13. Result of volumetry of VAT and SAT in whole-body CT images. The upper image shows a CT image in an umbilical slice, and the lower image shows extracted fat regions. The blue area represents SAT, and the red area represents VAT. The right table shows measurement results.

Table 3. Number of cases processed using CIRCUS CS (13 Jan. 2009 - 15 Aug. 2010).

CAD application	No. of cases
Cerebral aneurysm detection	2,564
Lung nodule detection	2,682
Skin lesion detection	7*
Vertebral deformity analysis	67*
Volumetry of VAT and SAT	654*

* Retrospective study

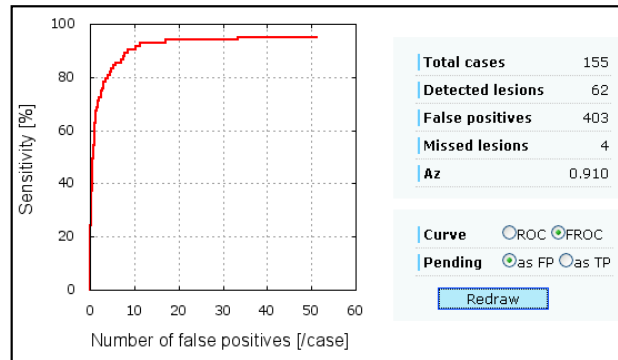


Fig. 14. Example of FROC curve for cerebral aneurysm detection.

number of cases processed using CIRCUS CS. At present, the feedback database includes 2,308 cases of cerebral aneurysm detection and 2,311 cases of lung nodule detection. Figure 14 shows an example of a free-response receiver operating characteristic (FROC) curve for cerebral aneurysm detection on the basis of accumulated clinical feedback. The number of FPs was 4.0 per case at 80% sensitivity. Figure 15 shows examples of scatter plots in lung nodule detection. From Fig. 15, individual differences in interpretation characteristics can be observed between two radiologists.

4 Discussion

The results show that CIRCUS DB has the potential to collect and register a sufficient number of clinical cases for CAD software development in a short period. However, the gold standard labeling of a large organ or region is still time-consuming. To reduce the time required for labeling a large organ or region, a labeling interface with interactive segmentation algorithms, such as the level set method [11] and graph cuts [12], is required.

CIRCUS CS makes it possible to use our CAD software in the daily clinical routine and to obtain feedback from radiologists. The method of clinical feedback in our system, which includes the classification of displayed candidates and

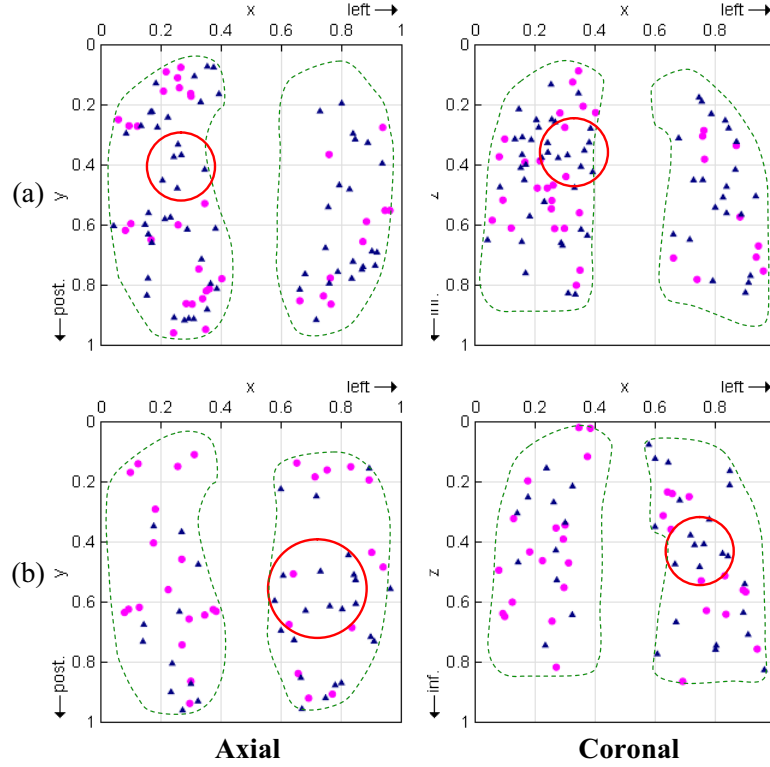


Fig. 15. Example of scatter plots in lung nodule detection. (a) Radiologist A with 14 years of experience; 125 cases, number of lesion candidates: 625. A higher tendency to overlook can be observed in the right pulmonary hilum (circle). (b) Radiologist B with 8 years of experience; 38 cases, number of lesion candidates: 190. A higher tendency to overlook can be observed in the left pulmonary hilum (circle). Dots represent known TPs, and triangles represent missed TPs.

the locations of FNs, makes it possible not only to evaluate the performance of the CAD software but also to improve the software. A few similar systems can be found in the literature such as in the report by Pietka et al. [13], which includes a workflow of the development, evaluation, and implementation of CAD software including an image database. One of the important original features of our platform is the function for collecting the personal diagnostic decisions of each radiologist, which is realized by the individual login. Collected data enable radiologists to check their own interpretation characteristics. In addition, it is possible to adjust the set of displayed candidates adaptively for each radiologist, such as by changing the criteria for displaying lesion candidates based on the tendency of radiologists to overlook lesions in specific regions. That is, a personalized CAD system optimized for each radiologist's interpretation characteristics

can be realized. This aspect is as important as improving the performance of the CAD software.

5 Conclusion

We have built an integrated platform for the development and assessment of various types of image analysis software, named CIRCUS. Our current works cover the implementation of an interface for the on-line learning of CAD software, and the tracking of longitudinal changes in performance by the refinement or adaptation of the CAD software in our system. A software toolkit of the web-based clinical server (CIRCUS CS) will be made publicly available after multicenter trials.

Acknowledgment

This study was partially supported by a Grant-in-Aid for Cancer Research from the Ministry of Health, Labour and Welfare, and a Grant-in-Aid and for Comprehensive Research on Aging and Health from the Ministry of Health, Labour and Welfare.

References

1. Pietka, E., Kawa, J.: Web oriented CAD architecture, *International Journal of Computer Assisted Radiology and Surgery*, 3, pp.S161–S162 (2008)
2. Le, A.H.T., Liu, B., Huang, H.K.: Integration of computer-aided diagnosis/detection (CAD) results in a PACS environment using CAD-PACS toolkit and DICOM SR. *International Journal of Computer Assisted Radiology and Surgery*, 4, pp.317–329 (2009)
3. Azevedo-Marques, P., Salomao, S.C., Traina, A.J.M., da Silva, M.P., Macedo, A.A., Pessotti, H.C.: CAD-PACS integration: a framework for pattern recognition of diffuse lung disease in HRCT. *International Journal of Computer Assisted Radiology and Surgery*, 4, pp.S180–S181 (2009)
4. Martinelli, M., Moroni, D., Salvetti, O., Tampucci, M.: A knowledge-based infrastructure for the management of diagnostic imaging procedures in the heart failure domain. *Transactions on Mass-Data Analysis of Images and Signals*, 2, pp.3–18 (2010)
5. Winter, L., Motal, Y., Docef, A.: On-line versus off-line accelerated kernel feature analysis: Application to computer-aided detection of polyps in CT colonography. *Signal Processing*, 90, pp.2456–2467 (2010)
6. Masumoto, T., Masutani, Y., Hayashi, N., Aoki, S., Mori H., Abe, O.: Automated detection system for cerebral aneurysm in magnetic resonance angiography: development and initial clinical experiences in multiple MRI scanners. In: *RSNA 2004 90th Scientific Assembly and Annual Meeting of Radiological Society of North America*, 2227NR-p (2004)

7. Nomura, Y., Nemoto, M., Masutani, Y., Maeda, E., Itoh, H., Hanaoka, S., Yoshikawa, T., Hayashi, N., Yoshioka, N., Ohtomo, K.: Computerized detection of pulmonary nodules based on dual classifiers for juxta-pleural and non-pleural nodules. *International Journal of Computer Assisted Radiology and Surgery*, 3, pp.S186–S187 (2008)
8. Nemoto, M., Nomura, Y., Masutani, Y., Hanaoka, S., Yoshikawa, T., Hayashi, N., Yoshioka, N., Ohtomo, K.: Development of ensemble based lesion detection method for body trunk FDG-PET/CT images. *International Journal of Computer Assisted Radiology and Surgery*, 4, pp.S190–S191 (2009)
9. Hanaoka, S., Nomura, Y., Nemoto, M., Masutani, Y., Maeda, E., Yoshikawa, T., Hayashi, N., Yoshioka, N., Ohtomo, K.: Automated segmentation method for spinal column based on a dual elliptic column model and its application for virtual spinal straightening. *Journal of Computer Assisted Tomography*, 34, pp.156–162 (2010)
10. DCMTK – DICOM Toolkit, <http://dicom.offis.de/dcmtdk.php.en>
11. Yang, J., Staib, L., Duncan, J.: Neighbor-constrained segmentation with level set based 3-D deformable models. *IEEE Transactions on Medical Imaging*, 23, pp.940–948 (2004)
12. Boykov, Y., Funka-Lea, G.: Graph cuts and efficient n-d image segmentation. *International Journal of Computer Vision*, 70, pp.109–131 (2006)
13. Pietka, E., Kawa, J., Spinczyk, D., Badura, P., Wieclawek, W., Czajkowska, J., Rudzki, M.: Role of radiologists in CAD life-cycle. *European Journal of Radiology* (2009), doi:10.1016/j.ejrad.2009.08.015